MODELLING MR DAMPERS UNDER NON-HARMONIC EXCITATIONS THROUGH LOGISTIC CURVE MODELS

Leonardo da Costa Rodrigues Ferreira[1], Marcus V. G. de Morais[2], Davi Matias Dutra da Silva [2]

[1]*Depto. Automotive Engineering, University of Brasília, Campus Gama*
Brasília/DF
leonardo.costa@aluno.unb.br
[2]*Depto. Mechanical Engineering, University of Brasilia, Campus Darcy*
mvmorais@unb.br, davimatiasbra@gmail.com
Brasília/DF

Abstract. The present work proposes modifications for a MR damper Sigmoid-curve-based mathematical model in the literature to expand the range of conditions in which it can be employed, such as white noise excitations, as well as increase its accuracy. The proposed formulation is compared to Bingham and Bouc-wen models, two formulations with widespread use for MR dampers. The Sigmoid model addressed some issues with prior models, such as their inaccuracy in situations where the current or excitation were continuously varied. However, this articles demonstrates that the model has stability issues, including instances of numerical divergence. This article proposes tweaks that eliminate the issue. It also further proposes an expanded model with more parameters based on the generalized logistic curve, evaluating if a better agreement between the numerical model and the experimental data is possible. The results are compared according to the sum of the absolute difference between the experimental and predicted force on steady-state conditions, where a lower value means a better agreement. The new model decreased the disagreement between the theoretical and numerical models by 8,6%. The modifications to address the numerical divergence were a success.

Keywords: MR damper, genetic algorithm, Bouc-wen, Bingham, Sigmoid rheological model

1 Introduction

Semi-active dampers are of interest to the automotive industry due to their good compromise between performance and cost, with the magneto-rheological (MR) dampers often used for this purpose due to their reliability (Soliman [1]). A few key characteristics that differentiate it from a normal damper are its strong non-linearity with respect to speed and its hysteretic behavior. These differences make numerical simulations of the damper complex, with many different models being used for modeling its behavior.

The Bingham model and its variants are often used to model MR dampers (Soltane et al [2], Fujitani et al [3], Sharma and Sharma [4]). As put by Rossi et al [5], the main draw point is that it's a reasonable approximation while being simple to model. There have been many variations of the model developed over the years, with Santade [6] having many examples of such cases. The Bouc-wen model has also been extensively used to model MR dampers (Ismail et al [7], Loh et al [8], Xiaomin et al [9], Zhu et al [10], Weber [11]), and according to Rossi et al [5] its main strength is modeling hysteretic behavior, with the drawback of having more parameters. Many examples of Bouc-wen models in the literature can be found in Kowk et al [12]. Lastly, the Sigmoid-inspired model has seen use (Wang et al (2001) [13], Silva et al [14], Ji et al [15], Yu et al [16]) due to its good agreement with the theoretical data, but it has the most parameters out of all these models.

In order to match the numerical model to a physical damper, it's necessary to perform a parametric identification on experimental data. For models with a high number of parameters, meta-heuristics algorithms are usually employed. The genetic algorithm (GA) is commonly used (Kowk et al [12], Yu et al [17], Zhu et al [10]) due to its capacity to converge to globally optimal solutions for non-linear problems with many parameters.

This work aims to propose two modifications to the Sigmoid-based rheological model proposed by Wang et

al (2004) [18]. The first is a modification to modify the damper behavior under non-harmonic excitations with non-ideal boundary conditions. The forces of the old and new proposed formulations are compared in different circumstances, demonstrating they're equivalent in test bench conditions but different otherwise, with the new proposal being more robust. The second is a modification to increase the model's precision. To evaluate the performance of the proposed extended model, the parametric identification of a MR damper for four different rheological models is performed, comparing their effectiveness at matching experimental data collected in a prior work by Silva et al [14]. Because of its desirable qualities and high presence in the literature, the parametric identification is done by means of a GA. The coefficients for each of the proposed models are found, as well as the adequacy of the fit.

2 Rheological models

2.1 Bingham body

There are many Bingham-inspired models in the literature, with the Bingham body model variant chosen over the simplest one due to the addition of a stiffness element. The Bingham body is a model that combines a Bingham plastic model in series with a linear spring element. The Bingham plastic is modeled as a damper in parallel with a dry friction element. The model is in Fig. (1).

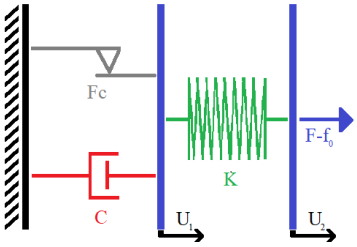

Figure 1. Bingham model.

The equations for the Bingham body model are given in Sapinski and Filus [19] apud Santade [6] as eq. (1).

$$\begin{cases} F = K(U_2 - U_1) + f_0 & if \quad |F| \leq F_c \\ F = C\dot{U}_2 + F_c + f_0 & if \quad |F| > F_c \end{cases} \tag{1}$$

where U is the displacement of the terminals, K is the linear spring constant, C is the linear damper constant, f_0 is a residual force, F_c is the dry friction force and F is the resulting damper force.

2.2 Bouc-wen

The Bouc-wen model is explained in Santade [6] as a linear stiffness element, a linear damper element, and a hysteresis Bouc-wen element, all in parallel, shown in Fig. (2). Kwok et al [12] gives the formulation for the

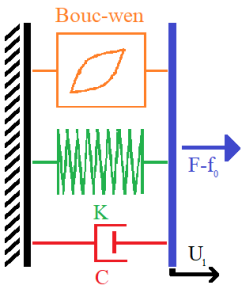

Figure 2. Bouc-wen model.

forces in a non-symmetric MR damper as well as the hysteretic component as such:

$$F = c\dot{x} + kx + \alpha z - f_0 \tag{2}$$

$$\dot{z} = (\delta - \gamma|\dot{z}|^n - \beta\dot{z}|\dot{z}|^{n-1})(\dot{x} - \mu\, sgn(x)) \tag{3}$$

where x is the displacement U, n, α, δ, γ, β and μ are the hysteresis loop constants, z is the hysteresis variable, f_0 is a residual force and c and k are the linear damping and stiffness of the model. The formulation used in Kwok et al [12] is chosen because it allows for force asymmetries to be accounted for.

Additionally, Erlicher and Point [20] report additional constraints that guarantee the model obeys the second law of thermodynamics. These conditions in eq. (4) will be respected in the parametric identification.

$$\begin{cases} n > 0 \\ \beta > 0 \\ -\beta \leq \gamma \leq \beta \end{cases} \tag{4}$$

2.3 Wang's model

Wang's model is a Sigmoid-curve-based model first described by Wang et al (2001) [13], with further developments to account for asymmetries described by Wang et al (2004) [18]. The final model described in the latter article is the one in eqs. (5,6,8,7).

$$F(\dot{x}) = f_t \frac{1 - e^{F_1(\dot{x})}}{1 + e^{F_1(\dot{x})}}(1 - k_5)(1 + F_2(\dot{x})) \tag{5}$$

$$f_t = f_0(1 + e^{a_1 v_m})\left(1 + \frac{k_2}{1 + e^{-a_2(i+I_0)}} - \frac{k_2}{1 + e^{-a_2(I_0)}}\right) \tag{6}$$

$$F_2(\dot{x}) = |(\dot{x})|e^{-a_4 v_m}\left(\frac{1 + sgn_2(\dot{x})}{2}k_{1c} + \frac{1 - sgn_2(\dot{x})}{2}k_{1e}\right) \tag{7}$$

$$F_1(\dot{x}) = -\frac{a_0}{1 + k_0 v_m}\left((\dot{x}) + sgn(\ddot{x})k_4 v_m(1 + \frac{k_3}{1 + e^{-a_3(i+I_1)}} - \frac{k_3}{1 + e^{-a_3(I_1)}}) + k_6 v_m\right) \tag{8}$$

where a_0, a_1, a_2, a_3, a_4, k_0, k_{1c}, k_{1e}, k_2, k_3, k_4, k_5, k_6, I_0, I_1 and f_0 are the model constants, i is the employed current and v_m is the peak velocity of the damper. The $sgn_2(\dot{x})$ function is a sign function that evaluates to +1 at 0.

2.4 v_m calculation and modification

Under harmonic excitations, the value of v_m is given by the expression in eq. (9), as given in Wang et al (2004) [18].

$$v_m = \omega\, a \tag{9}$$

Where ω is the excitation frequency and a is the amplitude. Under other excitations, Wang et al (2004) [18] suggests that the maximum velocity be calculated according to eq. (10), which yields the same result as eq. (9) under harmonic excitations.

$$v_m = \sqrt{\dot{x}^2 - \ddot{x}\, x} \tag{10}$$

However, this formulation leads to numerical issues under conditions that aren't test benches. An example of such condition is demonstrated in Fig. (3). U_1 now determines the values of x, $\dot{x}$ and $\ddot{x}$, but the forces exerted by Wang's damper modify U_1 too. As $\ddot{x}$ grows, so does v_m. Because $\ddot{x}$ also increases with e^{v_m}, this creates an exponential feedback loop. Numerical issues were experienced when attempting to simulate the system under such conditions, such as in quarter vehicle simulations, and a new formulation was sought out.

As a substitute term for v_m, eq. (11) is proposed.

$$\begin{cases} v_m = max(\dot{x}, v_m) & if \quad \ddot{x} \leq 0 \\ v_m = min(\dot{x}, v_m) & if \quad \ddot{x} > 0 \end{cases} \tag{11}$$

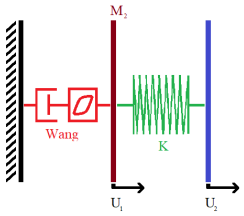

Figure 3. Example of Wang's damper under a different load condition.

This formulation has the same results as eq. (10) for steady-state under harmonic excitations, but avoids the issues with exponential feedback growth. It also depends only on past excitation conditions, thus eliminating responses to non-realized excitations such as the predicted future maximum velocity.

To demonstrate that the original v_m term is a source of instability under random loads and that the proposed formulation is equivalent under sinusoidal excitations, a comparison between simulations of the model in Fig. (3) with the two different formulations is performed.

2.5 Sigmoid curve modification

The general expression for the Sigmoid curve is also known as Richard's curve, and was first presented in Richards [21]. The general expression for the curve is given in eq. (12).

$$y = k_{cl} + \frac{K - k_{cl}}{(\gamma + Oe^{-Bt})^{\frac{1}{\eta}}} \tag{12}$$

The Sigmoid portion of eq. (6) is of the form of eq. (13).

$$y = f_t \frac{1 - e^{F_1(\dot{x})}}{1 + e^{F_1(\dot{x})}} = (K - k_{cl}) \frac{(C + O_1 e^{-Bt})^{\frac{1}{\eta}}}{(C + O_2 e^{-Bt})^{\frac{1}{\eta}}} \tag{13}$$

Where C, O_2 and η equal 1, O_1 equals -1, K equals f_t and k_{cl} equals 0. The coefficients set to 1, -1 and 0 could potentially be used to better the fit of the equations. As such, the modified form in eq. (14) is proposed.

$$F(\dot{x}) = f_t \frac{(\gamma - Oe^{F_1(\dot{x})})^{F_4(x)}}{(\gamma + Oe^{F_1(\dot{x})})^{F_4(x)}} (1 - k_5)(1 + F_2(\dot{x})) + k_{cl}\dot{x} \tag{14}$$

$$F_4(x) = \left(\frac{1 + sgn_2(\dot{x})}{2} \eta_p + \frac{1 - sgn_2(\dot{x})}{2} \eta_n \right)^{-1} \tag{15}$$

These equations give 5 additional degrees of freedom to the curve: O, k_{cl}, γ, η_n and η_p. Because the curve is asymmetric, the η coefficient was allowed to be asymmetric like the coefficient k_1 in the original formulation. The term k_{cl} was multiplied by $\dot{x}$ to make it a linear damping term instead. To assert whether this modification improves the model, a comparison fit was performed.

3 Parameters for v_m formulation and genetic algorithm

3.1 Genetic algorithm

The fitting of the function's coefficients was performed with the standard Matlab genetic algorithm (GA). As it's fitness criteria the cost function in eq. (16) was minimized. All simulations were performed using Matlab and Simulink routines.

$$C = \sum_{t=t_0}^{t_f} |F_{exp}(t) - F_{fcn}(X(t), h)| \tag{16}$$

Where C is the cost, $F_{exp}(t)$ is the experimental force measurement at time t, $F_{fcn}(x, t, h)$ is the expected force of the evaluated rheological model with coefficients h and excitation X(t) at time t, t_0 is the starting time and t_f is the finishing time. This formula is similar to ones used in the literature, such as by Kwok et al [2].

The start and finish times t_0 and t_f are chosen so as to guarantee that the system is under steady-state. The start time was 6 s and the finish time 98,6 s. The initial population was generated with a Sobol algorithm. The crossover rate was 80%, the elitism rate was 5% and the mutation rate was 15%.

3.2 Parameters of v_m formulation evaluation

For the comparison between the proposed v_m formulation expressions, the two models are ran under (1) a pure sinusoidal excitation with idealized terminals and (2) a white-noise added sinusoidal excitation under the conditions described in Fig. (3), hereby referred to as the under feedback condition. The parameters of the simulation are displayed in table (1). All simulations were performed using Matlab and Simulink routines.

Table 1. Parameters for the simulations for the v_m formulations.

Parameter	Sine amplitude	White noise power	Simulation duration	M_1	Individual numbers
Value	10^{-3}	1	100 s	1000	1080
Parameter	Model coefficients	Damper model	Initial x, $\dot{x}$ and $\ddot{x}$	K	Generations
Value	Table 5	Extended Sigmoid	0	1	300

4 Numerical results

The results for the sine-only excitations and white noise with feedback is in Fig. (4). The results for the optimization in the time domain and as a function of speed are in Fig. (5). The results for the optimization coefficients are in Tables (4), (5), (3) and (2). The results of the optimization are in Table (6).

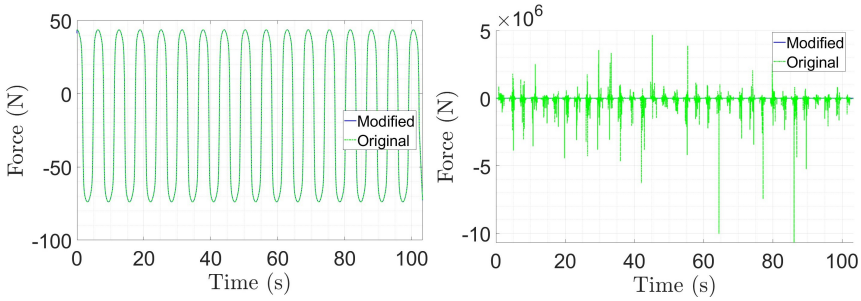

(a) Modified v_m, pure sine. (b) Modified v_m, feedback with noise.

Figure 4. Modified v_m formulation compared to original formulation, pure sine and sine with added white noise under feedback.

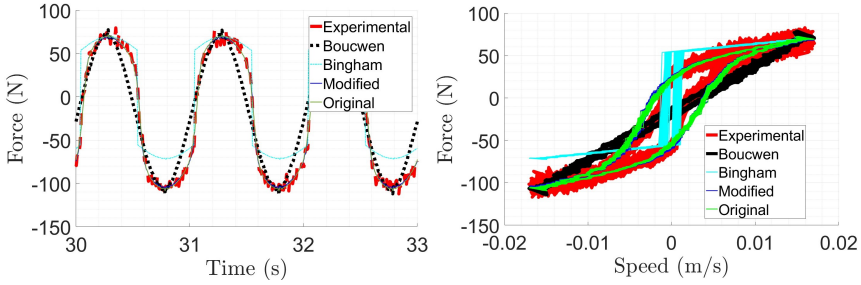

(a) Time domain results (b) Force as a function of speed.

Figure 5. Results for the rheological functions.

Table 2. Results for the fit of the Bingham rheological model.

Constant	c	f_c	k	f_0
Value	1004,74	54,56	$24,5 \cdot 10^3$	-0,91

Table 3. Results for the fit of the Bouc-wen rheological model.

Constant	n	α	δ	γ	λ	β	μ	f_0	c	k
Value	2.5·107	500,00	577,50	14,31	-8,01	21,06	-0.01	-9.04	5052,84	577,50

Table 4. Results for the fit of the original damper model from Wang et al (2001) [13].

Constant	Value	Constant	Value	Constant	Value	Constant	Value
a_0 (adm)	3,45·10^4	$a_4\ (m/s)^{-1}$	5.39	k_0 (adm)	3458.12	k_3 (adm)	1351.67
$a_1\ (m/s)^{-1}$	22.29	I_0 (amp)	-7.50	k_{1c} (adm)	67.38	k_4 (adm)	-0.1378
$a_2\ (amp)^{-1}$	0.038	I_1 (amp)	-1.10	k_{1e} (adm)	37.66	k_5 (adm)	0.3221
$a_3\ (amp)^{-1}$	-8.05	f_0 (N)	21.20	k_2 (adm)	1257.43	k_6 (adm)	6.93·10^{-3}

Table 5. Results for the fit of the new proposed damper model.

Constant	Value	Constant	Value	Constant	Value	Constant	Value
a_0 (adm)	3,45·10^4	$a_4\ (m/s)^{-1}$	10.46	k_0 (adm)	3356.67	k_3 (adm)	1335.20
$a_1\ (m/s)^{-1}$	23.94	I_0 (amp)	-10,96	k_{1c} (adm)	67.41	k_4 (adm)	-0.1377
$a_2\ (amp)^{-1}$	-35.44	I_1 (amp)	14,80	k_{1e} (adm)	36.52	k_5 (adm)	0.3221
$a_3\ (amp)^{-1}$	-4.33	f_0 (N)	21.21	k_2 (adm)	1257.43	k_6 (adm)	5.97·10^{-3}
$\eta_p\ (adm)$ and γ (adm)	1	η_n (adm)	1.13	O (adm)	0.9718	$k_{cl}(N \cdot s/m)$	44,10

Table 6. Equation (16) sum residuals.

Bingham	Bouc-wen	Wang et al (2004) [18]	Modified Exponential
29,8 ·10^4 N	22,85 ·10^4 N	7,07 ·10^4 N	6,46 ·10^4 N

4.1 Discussion

The results of the v_m modification demonstrate the three points proposed: the new formulation is equivalent to the old one under harmonic excitations at steady-state, the old formulation is unstable and diverges under white noise excitations with feedback, and the new formulation is stable and returns the expected results of a noisy sine.

For the expanded Sigmoid model, there was an improvement of 8,6% in the fit parameters over the old formulation. This improvement was seen as a result of the curve being able to better approximate the behavior at high velocities while maintaining it's shape at lower velocities. The Bingham and Bouc-wen models performed worse than both Sigmoid functions. Almost all added parameters were used, with the exception of γ, which was set to 1. The non-dimensional parameters varied little between the models, but the dimensional parameters were significantly altered.

5 Conclusions

The parameters for all four rheological models were found. The proposed extended Sigmoid model performed the best among the tested models, showing an improvement of $8,6\%$ over its literature counterpart. The optimization rejected the γ parameter. The new proposed formulation for calculating the v_m term showed itself to be stable under pure harmonic excitations as well as white noise added sinusoidal excitations. In contrast, the old formulation was demonstrated to be unstable and divergent for the latter case. These findings support the use of the new formulations for parametric identifications that desire greater accuracy, as well as simulations that use the MR damper under non test-bench conditions, such as vehicular simulations.

Authorship statement. The authors hereby confirm that they are the sole liable persons responsible for the authorship of this work, and that all material that has been herein included as part of the present paper is either the property (and authorship) of the authors, or has the permission of the owners to be included here.

References

[1] A. Soliman and M. Kaldas. Semi-active suspension systems from research to mass-market – a review. *Journal of Low Frequency Noise, Vibration and Active Control*, vol. 40, n. 2, pp. 1005–1023, 2021.
[2] S. Soltane, S. Montassar, O. B. Mekki, and R. E. Fatmi. A hysteretic bingham model for mr dampers to control cable vibrations. *Journal of mechanics of materials and structures*, 2015.
[3] H. Fujitani, H. Sodeyama, T. Tomura, T. Hiwatashi, Y. Shiozaki, K. Hata, K. Sunakoda, S. Morishita, and S. Soda. Development of 400kN magnetorheological damper for a real base-isolated building. In G. S. Agnes and K.-W. Wang, eds, *Smart Structures and Materials 2003: Damping and Isolation*, volume 5052, pp. 265 – 276. International Society for Optics and Photonics, SPIE, 2003.
[4] S. K. Sharma and R. C. Sharma. Simulation of quarter-car model with magnetorheological dampers for ride quality improvement. *International Journal of Vehicle Structures Systems*, 2018.
[5] A. Rossi, F. Orsini, A. Scorza, F. Botta, N. Belfiore, and S. Sciuto. A review on parametric dynamic models of magnetorheological dampers and their characterization methods. *Actuators*, vol. 7, pp. 16, 2018.
[6] F. Santade. Análise dinâmica de amortecedores não lineares assimétricos, com histerese e sujeitos a folga e avaliação do efeito temperatura. Master's thesis, Universidade Estadual Paulista, 2017.
[7] M. Ismail, F. Ikhouane, and J. Rodellar. The hysteresis bouc-wen model, a survey. *Archives of Computational Methods in Engineering*, vol. 16, pp. 161–188, 2009.
[8] C.-H. Loh, L. Wu, and P.-Y. Lin. Displacement control of isolated structures with semi-active control devices. *Journal of Structural Control*, vol. 10, pp. 77 – 100, 2003.
[9] X. Xue, L. Zhang, and Q. Sun. Parameter identification and simulation of the noise-involved hysteretic model using improved genetic algorithm. In *2010 International Conference on Measuring Technology and Mechatronics Automation*, volume 2, pp. 868–871, 2010.
[10] H. Zhu, X. Rui, F. Yang, W. Zhu, and M. Wei. An efficient parameters identification method of normalized bouc-wen model for mr damper. *Journal of Sound and Vibration*, vol. 448, pp. 146–158, 2019.
[11] F. Weber. Bouc–wen model-based real-time force tracking scheme for mr dampers. *Smart Materials and Structures*, vol. 22, n. 4, pp. 045012, 2013.
[12] N. Kwok, Q. Ha, M. Nguyen, J. Li, and B. Samali. Bouc–wen model parameter identification for a mr fluid damper using computationally efficient ga. *ISA Transactions*, vol. 46, n. 2, pp. 167–179, 2007.
[13] E. R. Wang, X. Q. Ma, S. Rakheja, and C. Y. Su. Modeling asymmetric hysteretic properties of an mr fluids damper. *43rd IEEE Conference on Decision and Control*, 2004.
[14] D. M. D. d. Silva, S. M. Ávila, and M. V. G. d. Morais. Sistema de suspensão semi-ativa automotiva utilizando amortecedor magneto-reológico, 2022.
[15] H. Ji, Y. Huang, S. Nie, F. Yin, and Z. Dai. Research on semi-active vibration control of pipeline based on magneto-rheological damper. *Applied Sciences*, vol. 10, n. 7, 2020.
[16] J. Yu, X. Dong, and Z. Zhang. A novel model of magnetorheological damper with hysteresis division. *Smart Materials and Structures*, vol. 26, n. 10, pp. 105042, 2017a.
[17] J. Yu, X. Dong, and Z. Zhang. A novel model of magnetorheological damper with hysteresis division. *Smart Materials and Structures*, vol. 26, n. 10, pp. 105042, 2017b.
[18] X. Q. Ma, E. R. Wang, S. Rakheja, and C.-Y. Su. Modeling hysteretic characteristics of mr-fluid damper and model validation. In *Proceedings of the 41st IEEE Conference on Decision and Control, 2002.*, volume 2, pp. 1675–1680 vol.2, 2002.
[19] B. Sapiński and J. Filuś. Analysis of parametric models of mr linear damper. *Journal of Theoretical and Applied Mechanics*, vol. 41, 2003.
[20] S. Erlicher and N. Point. Thermodynamic admissibility of bouc–wen type hysteresis models. *Comptes Rendus Mécanique*, vol. 332, n. 1, pp. 51–57, 2004.
[21] F. J. RICHARDS. A Flexible Growth Function for Empirical Use. *Journal of Experimental Botany*, vol. 10, n. 2, pp. 290–301, 1959.